

# Low Intensity Ultrasound as a Probe to Elucidate the Relative Follicular Contribution to Total Transdermal Absorption

V. M. Meidan,<sup>1</sup> M. Docker,<sup>2</sup> A. D. Walmsley<sup>3</sup>,  
and W. J. Irwin<sup>1,4</sup>

Received June 17, 1997; accepted October 6, 1997

**Purpose.** To investigate the effect of ultrasound on the histological integrity and permeability properties of whole rat skin *in vitro*.

**Methods.** A defined, field-free source of ultrasound was used to irradiate excised rat skin prior to *in vitro* transport studies in Franz-type cells using sucrose, mannitol, hydrocortisone, 5-fluorouracil and aminopyrine.

**Results.** High intensity ultrasound irradiation (1 to 2 W cm<sup>-2</sup>) irreversibly damaged cutaneous structures and increased the percutaneous transport rate of permeants. In contrast, skin integrity was largely maintained with low intensity ultrasound (0.1 to 1 W cm<sup>-2</sup>) which merely discharged sebum from the sebaceous glands so as to fill much of the hair follicle shafts. This effect caused the transfollicular absorption pathway to be blocked for hydrophilic molecules that penetrate *via* this route and reduced the transport rate significantly.

**Conclusions.** This phenomenon may be used as a probe to elucidate the relative follicular contribution to total penetration for hydrophilic permeants. It was demonstrated that the shunt pathway was responsible for virtually all mannitol and sucrose penetration, perhaps half of hydrocortisone transport but negligible aminopyrine and 5-fluorouracil penetration.

**KEY WORDS:** Follicular transport; mechanism; percutaneous absorption; phonophoresis.

## INTRODUCTION

Phonophoresis (sonophoresis) is the use of ultrasound to enhance percutaneous drug delivery. Ultrasound may potentially accelerate drug absorption *via* several mechanisms such as heating, radiation pressure, acoustic microstreaming or cavitation. However, there have been mixed reports on the effectiveness of this procedure; some workers have reported that ultrasound can significantly enhance percutaneous drug absorption whilst other groups have found ultrasound to have no effect whatsoever (1). Much of the literature on phonophoresis suffers from the defect of inadequate dosimetry of the ultrasound source which is often due to complex and unpredictable standing wave patterns occurring within the experimental assemblage (2). This major limitation has added to the confusion in this area.

The aim of this study was to determine the effect of ultrasound on the structural morphology and barrier properties of whole rat skin *in vitro*. An exposure system was specially developed so that the skin was exposed to a definable ultrasonic field with no standing waves. This is termed an ultrasound free-field. It was convenient to classify effects into those produced by low intensity ultrasound (<1 W cm<sup>-2</sup>) and high intensity ultrasound (1 to 2 W cm<sup>-2</sup>) respectively. In order to elucidate the nature of any ultrasound-induced perturbations, a heat-alone control application was devised which simulated the ultrasonic heating effect without generating mechanical forces. In addition to histological analysis, control and sonicated rat skin samples were also used as barriers for percutaneous absorption experiments involving sucrose, mannitol, 5-fluorouracil, aminopyrine, and hydrocortisone. These compounds encompass a variety of octanol-water partition coefficients ranging from log -2.6 to log 1.55 and may be expected to show a variation in percutaneous penetration ranging from transfollicular (hydrophilic compounds) to transcellular (more hydrophobic compounds).

## METHODS

### Development of the Ultrasonic Free-Field Exposure System

In order to subject skin samples to an ultrasonic free-field, a suitable exposure system had to be initially designed. The simplest such system involves placing the skin section flat on a sheet of clingfilm, stretched taught over a water-filled beaker. If the beaker is composed or lined with sound-absorbing material then this attenuates the incoming energy and prevents standing wave development. Initially, a plastic beaker (d = 12 cm; h = 12 cm) was investigated for its sound-absorbing properties. To this end, a 3.5 MHz reversible transducer (595522B, 19 mm, Long I. F. Series L, A71110Hr, Picker International, Cleveland, Ohio) was used in conjunction with an A-mode scan (Clinical Diagnostic, Series 4100MG, Kretz-Technik AG, Zipf, Austria). This equipment essentially acts as a reversible piezoelectric transducer, emitting a brief pulse of ultrasound and then recording the energy of any returning ultrasonic echo (3). The plastic beaker was filled with water and the transducer of the A-scan was then placed just below the water surface, with its radiating surface pointing downwards toward the base of the container. Since ultrasound undergoes almost total reflection at a stainless steel-water interface, the acoustic reflectivity of a stainless steel beaker was similarly measured in order to obtain a reference reading representing virtually 100% reflection. It was determined that the plastic-water interface reflected back approximately 10% of the energy. In order to develop a more sound-absorptive system, the echo tests were repeated with the beaker entirely lined on all its inside surfaces with sections of thick-pile carpet. Common household carpet has been used for many years as an inexpensive, readily available, ultrasound-absorbing material (4). The carpet lining had to be left submerged in water for 10 min so as to permit entrapped air to escape to the water surface. It was determined that the carpet lining absorbed at least 99% of the incoming acoustic beam and that the reflected energy component was therefore negligible. Consequently, it was decided to employ the carpet-lining for the free-field exposure system. Further tests with the A-scan

<sup>1</sup> Pharmaceutical Sciences Institute, Aston University, Aston Triangle, Birmingham, B4 7ET, United Kingdom.

<sup>2</sup> Birmingham Maternity Hospital, Queen's Park Road, Edgbaston, Birmingham, B15 2EG, United Kingdom.

<sup>3</sup> School of Dentistry, University of Birmingham, St. Chad's Queensway, Birmingham, B4 6NN, United Kingdom.

<sup>4</sup> To whom correspondence should be addressed. (e-mail: w.j.irwin@aston.ac.uk)

demonstrated that tiny variations in the angle made by the transducer with the water did not greatly affect the magnitude of the reflections, thus indicating that holding the transducer by hand would be acceptable. A sheet of cling film was stretched taut over the surface of the water and secured with rubber bands. This provided a physical base to support the skin samples to be sonicated. Coupling gel (Henleys Medical Supplies, Welwyn Garden City, UK), exhibiting a low attenuation coefficient, was applied to make contact between the transducer, skin and cling film. Figure 1 depicts the ultrasound free-field exposure system developed for these studies.

#### Development of the Heat-Alone Exposure Protocol

Initially, an ultrasonic free-field of intensity  $1.5 \text{ W cm}^{-2}$  was beamed across samples of whole rat skin by using the beaker assembly shown in Figure 1. After the 5 min application period, the skin surface temperature at the centre of the sonicated region was measured by thermocouple and was found to be  $42^\circ\text{C}$ . An aluminium and perspex cylinder ( $d = 3.7 \text{ cm}$ ;  $l = 6 \text{ cm}$ ; approximately the same surface area as the large transducer) was subsequently employed to simulate the heating effect of the  $1.5 \text{ W cm}^{-2}$  ultrasonic output. The hollow interior of the probe, was connected by rubber tubing to a thermostatically controlled water pump (Churchill-Matrix, Churchill Instrument Company Ltd., Perivale, UK). When the pump was switched on, the circulating hot water heated the aluminium probe towards an equilibrium temperature. When the thermostat indicated that the desired temperature had been attained, the cylinder was employed to heat skin samples on the carpet-lined beaker using the same technique as described for the ultrasound transducer. Due to inefficiencies in heat conduction within the system, the actual temperature at the skin surface, in the centre of the probe-exposed area, was slightly lower than that indicated by the thermostat dial. Therefore, the heating probe was pre-calibrated with a differential thermocouple (3202 type K,  $d = 1 \text{ mm}$ ; Digitron Instruments Ltd., Hertford, UK) and it was determined that the skin temperature was approximately 10% lower than that indicated by the thermostat. Therefore, the thermostat dial was set to  $46^\circ\text{C}$  in order to produce a final skin surface temperature of  $42^\circ\text{C}$ . It should be noted that temperature readings at specific points can only give an indication of total heat generated. The temperature distribution throughout the skin is inhomogeneous due, for example, to spatial fluctuations in the output intensity and partial reflections at the interfaces between the skin strata.

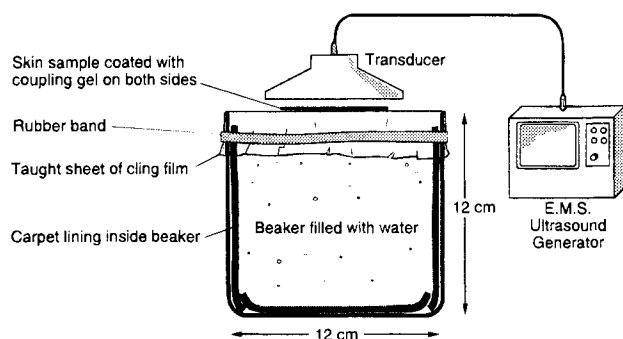


Fig. 1. Beaker assembly employed as an ultrasound free-field.

#### Transport Studies

Whole skin was obtained from male Wistar rats, 4 to 5 months old and weighing 250 to 300 g. The animals were sacrificed by cervical dislocation and the dorsal region of each rat was shaved with electric clippers (Model no.50, Sunbeam-Oster, Oxfordshire, UK). A pair of scissors was used to excise a sheet of whole-thickness intact skin from the back of each animal. Adhering fat and other visceral debris were removed from the undersurface of this skin. The isolated skin was cut into 6 rectangular sections of tissue (side length, 2 to 3 cm). These skin samples were either used immediately as barrier membranes, or alternatively stored at  $-20^\circ\text{C}$  between sheets of aluminium foil for a period of up to 1 month (5). Each skin section was coated with 0.5 g of ultrasound coupling gel (Henley's Medical Supplies Ltd., Welwyn Garden City, UK) on the inner surface and 1 g of gel on the outer surface. The skin sample was placed flat upon the sheet of cling film comprising one of the two exposure systems described above (*i.e.* ultrasound or heat-alone). For the ultrasound-exposure regime, the large transducer of an ultrasound generator (Therasonic 1032, model no. 50, EMS Greenham Ltd., Wantage, Oxfordshire) was placed on top of the sample so that the skin was compressed flat between the transducer and the cling film. A 1.1 MHz frequency was selected and the generator was switched on at a set intensity (0, 0.1, 1, 1.5, 1.75 or  $2 \text{ W cm}^{-2}$ ). The transducer was hand-held perpendicular to the skin surface for 5 min whilst the skin was sonicated. The area of skin exposed to the ultrasound was  $4.4 \text{ cm}^2$  while the active area of the penetration chamber varied from 2.2 to  $3.3 \text{ cm}^2$ . For the heat-alone studies, the aluminium heating probe was similarly used to heat the skin samples to a central surface temperature of  $42^\circ\text{C}$  over 5 min (mimicking the thermal effect of  $1.5 \text{ W cm}^{-2}$  ultrasound). Following sonication or direct heating, the skin sections were repeatedly washed with distilled water and dried with a paper towel in order to remove residues of coupling gel. Subsequently, the sections were mounted on Franz diffusion cells jacketed at  $37^\circ\text{C}$  (6). The receptor volumes varied from 24 to 33 ml; and sample aliquots were 1.1 ml. In these permeation experiments, the donor phase consisted of 100 ml of ethanolic solution containing 5% v/v of the appropriate radiolabelled drug. The drugs were [ $^{14}\text{C}$ ]-sucrose (1,819 pmol, 0.0370 MBq, Amersham International Plc, Amersham, UK); [ $^{14}\text{C}$ ]-mannitol (17,874 pmol, 0.0370 MBq, Amersham International Plc); [ $^3\text{H}$ ]-hydrocortisone (63.36 pmol, 0.1850 MBq, Amersham International Plc); [ $^3\text{H}$ ]-5-fluorouracil (333.3 pmol, 0.1628 MBq, NEN Life Science Products, Hounslow, UK); and [ $^3\text{H}$ ]-aminopyrine (2313 pmol, 0.0093 MBq, Amersham International Plc). The composition of the receptor phase depended upon the nature of the penetrant. For sucrose, mannitol, 5-fluorouracil and aminopyrine, the receptor solution was distilled water but for hydrocortisone, 5% v/v aqueous ethanol was employed. In either case, the solutions were partially degassed by heating to  $38^\circ\text{C}$  and then sonicated in an ultrasound bath (Kerry, Pulsatron 125) for 3 min.

The permeation experiment was allowed to proceed for 5 h during which 1.1 ml aliquots of receiver solution were withdrawn at 30 min intervals and replaced by an identical volume of drug-free solution. Each 1.1 ml sample was vortexed which 10 ml of scintillation fluid (Optiphase Hisafe 3, Fisher Chemicals, Loughborough, UK) and the emitted activity was counted

in a liquid scintillation counter (Packard 1900T.R, Packard, Pangbourne, UK). The activity values were converted to drug concentration values according to the activity/mole ratio of each radiolabelled drug. These drug concentration values were corrected for progressive dilution using equation 1 (7):

$$M_t(n) = V_r \cdot C_n + V_s \cdot \sum_{m=1}^{n-1} C_m \quad (1)$$

where  $M_t(n)$  is the current cumulative mass of drug transported across the membrane at time  $t$ ,  $C_n$  represents the current concentration in the receiver medium and  $\sum C_m$  denotes the summed total of the previous measured concentrations [ $m = 1$  to  $(n - 1)$ ];  $V_r$  is the volume of the receiver medium and  $V_s$  corresponds to the volume of sample removed for analysis. The amount of drug penetrating the skin per unit area was obtained by dividing the obtained concentrations by the surface area available for diffusion and this value was different for each individual Franz cell. Each permeation experiment was conducted in triplicate.

### Histological Techniques

In order to view the gross morphological changes associated with exposure to high intensity ultrasound ( $1$  to  $2 \text{ W cm}^{-2}$ ), a regular wax-embedding method was employed in conjunction with eosin and haematoxylin staining. This involved cutting out strips ( $1 \text{ cm} \times 3 \text{ mm}$ ) from skin samples that had been sonicated or heated. Following fixation in 4% neutrally buffered formalin (0.4% w/v sodium dihydrogen orthophosphate, 0.65% w/v disodium hydrogen orthophosphate and 4% v/v formaldehyde), the strips were dehydrated and cleared in an enclosed automatic tissue processor (Shandon Hypercenter 2, Life Sciences International (UK) Ltd., Basingstoke, UK). The skin strips were then wax-impregnated with paramat wax (Merck Ltd., Poole, UK) under vacuum. These samples were blocked out in molten paraffin wax delivered by an automated wax dispensing machine (Boova 39 Professional Embedding Centre, Klanestaff, Tenbury Wells, UK). A base sledge microtome (IS300 Anglia Scientific, Life Sciences International (UK) Ltd., Basingstoke, UK) was employed to cut 5 mm-wide transverse tissue sections. These sections were placed on glass slides and dried for 10 min at  $60^\circ\text{C}$  in a slide dryer (Luckham Model SD350, Life Sciences International (UK) Ltd., Basingstoke, UK). The skin samples were stained with Gill's haematoxylin and eosin dye and mounted on a microscope slide. Finally, the mounted sections were photographed with a camera (Olympus PM6, Olympus Optical Company (UK) Ltd., London, UK) attached to a microscope (Olympus BH, Olympus Optical Company (UK) Ltd.) set at  $\times 100$  magnification. For those skin sections that had been exposed to low intensity ultrasound ( $0.1$  or  $1 \text{ W cm}^{-2}$ ), it was necessary to employ a more sensitive histological procedure that maintains the distribution of endogenous lipids in the skin samples. To this end, three strips of tissue, ( $\sim 8 \text{ mm} \times 4 \text{ mm}$ ) were dissected from the central area of each exposed skin section. The strips of tissue were frozen on their sides on small pieces of cardboard by immersion in liquid nitrogen. The frozen tissue strips were sprayed with a cooling aerosol ("Freeze-it" E-series, Life Sciences International (UK) Ltd.) and transferred to an automated freezing microtome (Anglia Scientific 600 Cyrotome, Life Sciences International (UK) Ltd., Basingstoke, UK) pre-equilibrated at a temperature of  $-28^\circ\text{C}$ . An adhesive gel (Cyro-M-Embedding Compound, Bright

Instruments Ltd., Cambridge, UK) was used to embed the strips of skin into the requisite position within the microtome chamber. The microtome was used to produce several sections, each with a thickness of 9  $\mu\text{m}$ , from each tissue strip and these were fixed for 1 h in neutrally buffered formalin. Subsequently, these sections were immersed for 15 min in a working solution of Oil Red O and subsequently differentiated in 60% isopropanol (8). The skin samples were then counterstained for 3 min with several drops of Mayer's haemalum. This agent was then removed by rinsing in distilled water. Finally, the mounted sections were photographed with a camera (Olympus OM-4, Olympus Optical Company (UK) Ltd.) attached to a microscope (Jenamed, Zeiss, Germany) set at  $\times 125$  magnification.

## RESULTS AND DISCUSSION

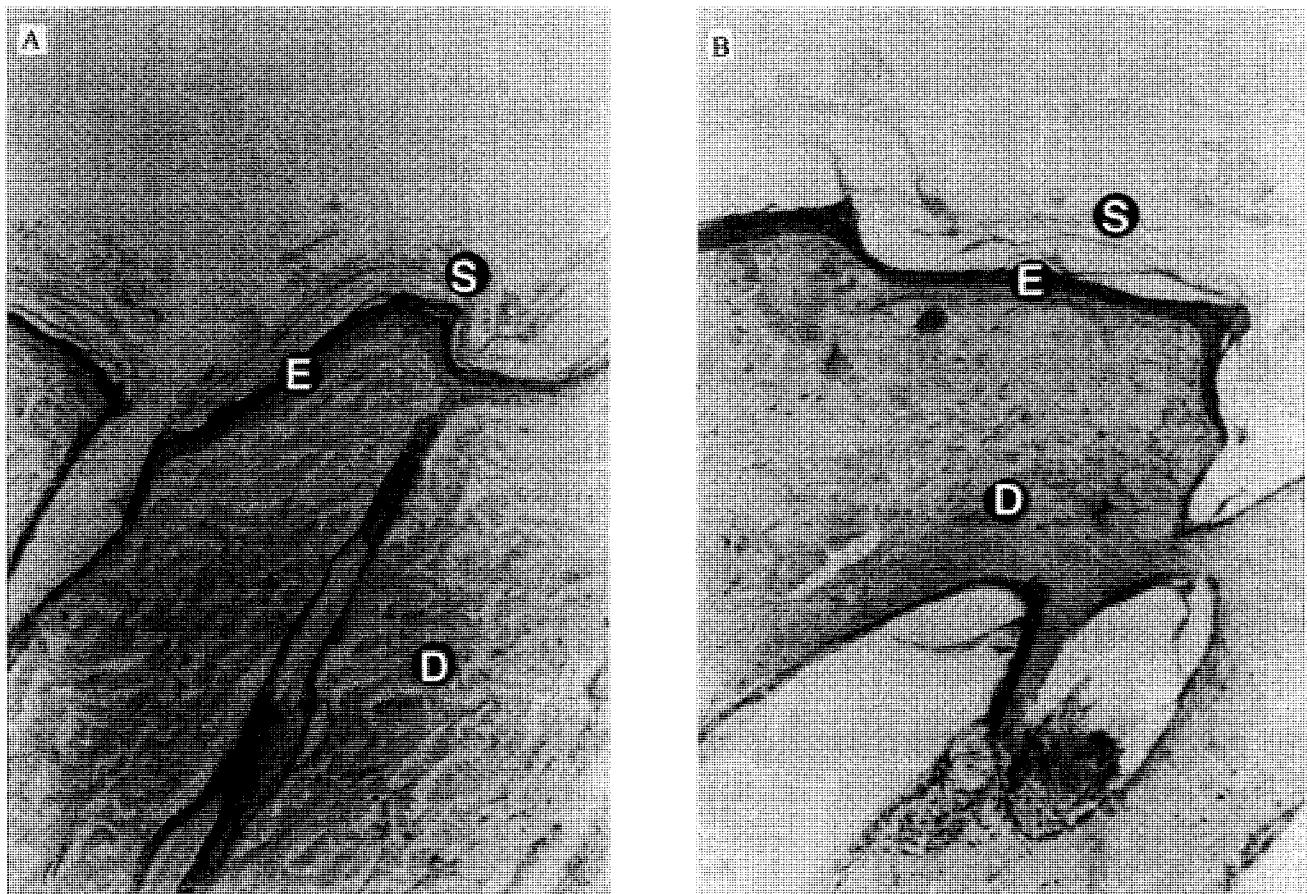
### Histological Changes Following Sonication at High Intensities

Figure 2A shows a section through a control sample of rat skin. The stratum corneum can be discerned as feint, wavy lines (S); the viable epidermis is stained reddish brown (E); while the dermal protein appears light brown (D). The nucleated cells of the sebaceous glands and epidermis can also be distinguished. The apparently empty spaces within the dermis are an artefact of the sectioning process. The only detectable change in the skin following exposure to  $1 \text{ W cm}^{-2}$  ultrasound was perhaps a slight thinning of the stratum corneum. Following sonication at  $1.5 \text{ W cm}^{-2}$ , however, significant morphological alterations were observed at the central site of each skin sample where the energy deposition was greatest. Here, ultrasound had detached the cornified layer from the epidermis and, furthermore, it had produced congealing of the dermal tissue. Presonication at  $1.75 \text{ W cm}^{-2}$  and  $2 \text{ W cm}^{-2}$  produced complete stratum corneum removal and dermal degeneration throughout virtually the whole area of the exposed skin (Figure 2B). Very similar patterns of progressive injury have been reported in other ultrasound-application studies involving live male Wistar rats (9). These workers applied 1 MHz ultrasound, through a layer of coupling gel, to the abdominal skin of anaesthetised animals *in vivo*. Following 10 min of sonication, whole skin samples were removed and subjected to haematoxylin and eosin staining. At intensities of up to  $0.5 \text{ W cm}^{-2}$ , the skin was histologically unaltered. Minor epidermal atrophy and collagen fibre degeneration were first observed at  $0.75 \text{ W cm}^{-2}$  and these detrimental changes progressed to large scale necrosis as the beam intensity was amplified.

In order to determine to what extent the morphological perturbations observed were an artefact of the thermal effects of ultrasound, a cylinder heated the skin specimens by simple conduction to a central surface temperature of  $42^\circ\text{C}$ . This is equivalent to the final surface temperature produced by the  $1.5 \text{ W cm}^{-2}$  beam. This heat-alone treatment did not affect the microscopic appearance of the skin. This suggests that the mechanical forces of the  $1.5 \text{ W cm}^{-2}$  beam may have contributed substantially to the observed changes in skin structure.

### Histological Changes Following Sonication at Low Intensities

Figure 3A shows a photomicrograph of a control section of whole rat skin stained with Oil Red O. Unsaturated hydrophobic



**Fig. 2.** Transverse section through control skin (A) and through skin sonicated at  $2 \text{ W cm}^{-2}$  (B) showing detachment of the stratum corneum and dermal degeneration (S, stratum corneum; E, epidermis; D, dermis; scale 1:167).

lipids, including fatty acids, esters and non-saponifiable lipids have been stained red (L). The nucleated cells of the epidermis (N) and sebaceous glands have been stained blue and hence these structures can be readily distinguished. It can be seen that in the absence of ultrasound, the unsaturated, hydrophobic lipids were predominantly concentrated within the cells of the sebaceous glands so as to almost entirely fill these structures. The hair follicle shaft was relatively free of dyed lipids. It can be seen that pre-sonication at  $0.1 \text{ W cm}^{-2}$  resulted in the transport of these lipids out of much of the sebaceous gland so that they filled all of the hair follicle shaft, right up to the skin surface (Figure 3B). The same process was observed following exposure to  $1 \text{ W cm}^{-2}$  ultrasound. This phenomenon has not been previously described in any of the literature reports.

Heat, by virtue of the application of ultrasound is unlikely to be causing the sebum transfer effect as the application of  $0.1 \text{ W cm}^{-2}$  ultrasound, in control experiments, resulted in a negligible surface temperature increase. Consequently, it is more probable that mechanical forces are responsible. The sebaceous glands may be being compressed during the positive pressure phases of the acoustic wave, thus promoting the discharge of lipid. However, since the sebaceous glands are much smaller than the ultrasonic wavelength, a difference in acoustic pressure, at any one instance, across the gland cannot be causing the effect. Alternatively, second-order effects such as microcurrents and stable cavities developing within or in the vicinity

of the sebaceous gland could cause sebum release via a yet unknown mechanism.

Although the heating component of low intensity ultrasound ( $0.1 \text{ W cm}^{-2}$ ) was probably not responsible for lipid release, simple heating to a surface temperature of  $42^\circ\text{C}$  did cause lipid release. Heating of the sebaceous gland produces a consequent thermodynamic increase in its internal pressure, thus promoting the release of its contents. The lipid release patterns produced by ultrasound and heat alone were visually indistinguishable (cf Figure 3B). This suggests that both the thermal and mechanical effects of ultrasound can discharge lipids from the sebaceous glands. The mechanical forces dominate at lower intensities but both attributes operate at higher intensities ( $1$  to  $2 \text{ W cm}^{-2}$ ). Transport through the heat-treated barrier was too low for reliable quantification.

### Percutaneous Absorption Studies

#### Sucrose

The sucrose permeation profiles, representing the influence of control ( $0 \text{ W cm}^{-2}$ ), low intensity ( $0.1 \text{ W cm}^{-2}$ ) and high intensity ( $2 \text{ W cm}^{-2}$ ) ultrasound are shown in Figure 4 and Table 1. The absorption of sucrose through non-sonicated skin can be described in terms of 3 distinct stages. There is an initial mean lag-time of just over 1 h. This is followed by a mean

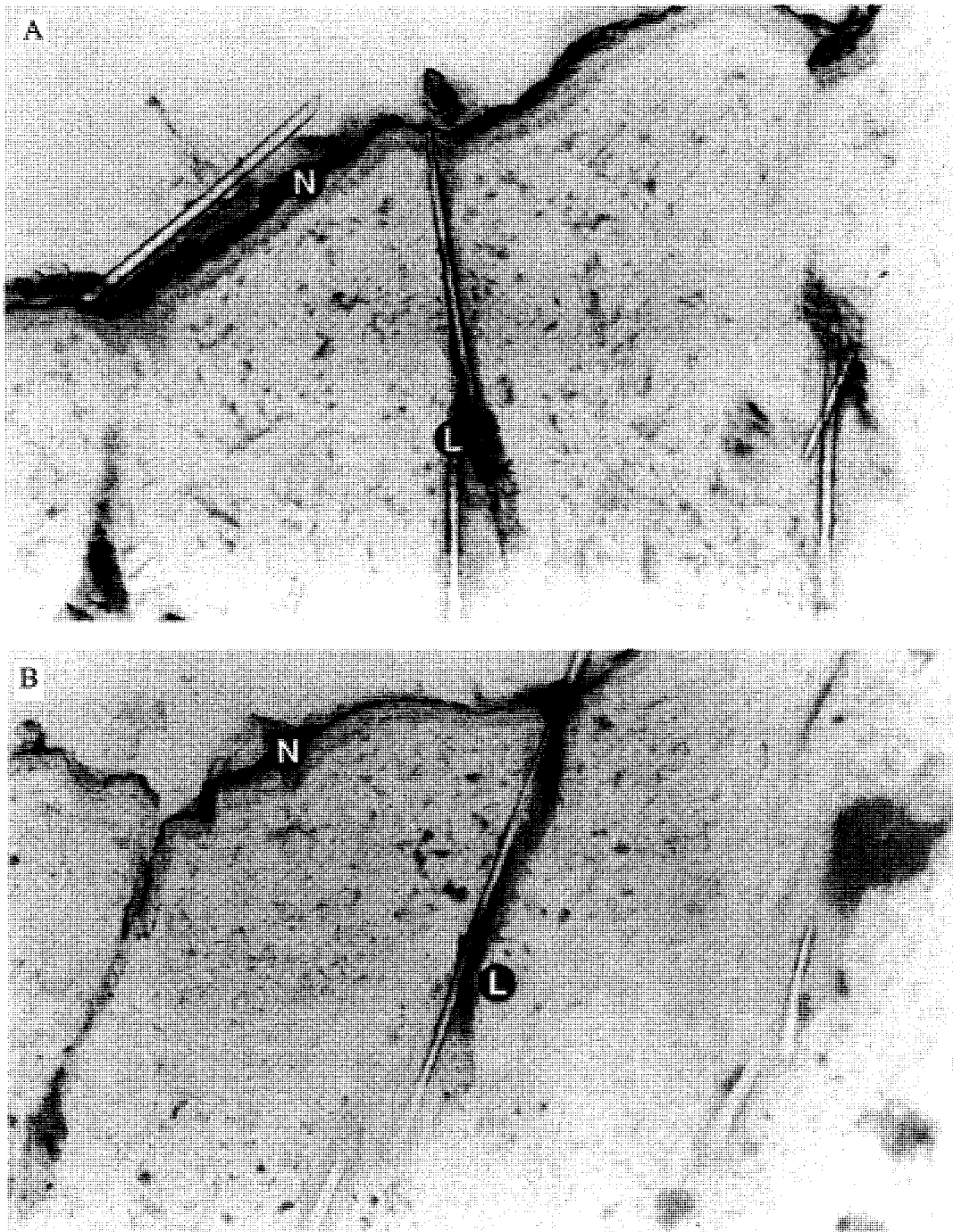


**Fig. 3.** Oil-Red-O stained section through non-sonicated skin showing sebum concentrated within the sebaceous gland (A) and through skin sonicated at  $0.1 \text{ W cm}^{-2}$  (B) showing sebum deposition within the hair follicle shafts; (L, hydrophobic lipids; N, nucleated epidermis; scale 1:200). Oil-red-O interacts with the hydrophobic lipid fractions that are liquid or semi-solid at room temperature. Since the lipid melting point depends upon the number of double bonds in the molecule temperature, all unsaturated fatty acid acids, esters and non-saponifiable lipids are stained. Mayer's Haemalum stains nucleic acids. The red, lipid-stained regions (dark areas associated with the hair follicles in the figure) are essentially found towards the base of the hair follicles and indicate the position of the sebaceous gland.

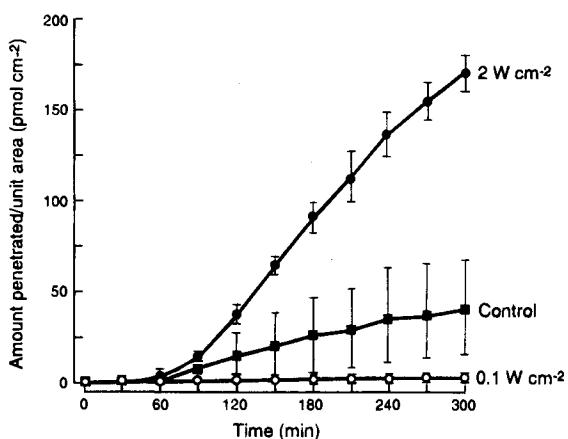


Fig. 4. The effect of presonication on sucrose penetration through rat skin (■, control,  $n = 4$ ; ◆,  $0.1 \text{ W cm}^{-2}$ ,  $n = 3$ ; ●,  $2 \text{ W cm}^{-2}$ ,  $n = 3$ ).

linear flux of  $11.49 \text{ pmol cm}^{-2} \text{ h}^{-1}$  ( $k_p = 6.31 \times 10^{-4} \text{ cm h}^{-1}$ ). Since sucrose is generally considered too hydrophilic to diffuse through the bulk stratum corneum ( $\text{Log } P = -2.4$ ), this transport is most likely to be mediated *via* a transfollicular route. From 4 h onwards, there is a plateau indicating that penetration has stopped. This occurs because the ethanol evaporates from the skin surface causing a fall in the hydrodynamic force necessary to drive sucrose through this transfollicular pathway.

The application of high intensity ultrasound ( $2 \text{ W cm}^{-2}$ ) increased sucrose flux to  $51.36 \text{ pmol cm}^{-2} \text{ h}^{-1}$  ( $k_p = 28.23 \times 10^{-4} \text{ cm h}^{-1}$ ). At this intensity, ultrasound totally detached the stratum corneum from the epidermis (Figure 2B). The removal of the lipoidal barrier allows sucrose to directly diffuse into the underlying hydrophilic layers of the epidermis and dermis. The resulting high penetration rate rapidly depleted the donor compartment ( $1,819 \text{ pmol}$ ) of sucrose. Therefore, from 2.5 h onwards, the penetration rate progressively decreased.

Presonication at a low intensity ( $0.1 \text{ W cm}^{-2}$ ) resulted in a virtually complete inhibition of sucrose permeation. It has already been established that low intensity ultrasound discharges sebaceous lipids into the hair follicle shaft and that furthermore, sucrose penetration is mediated *via* a transfollicular pathway. Consequently, it follows that the hair follicle shafts

constitute that transfollicular route. The horny layer is absent over much of the inner surface of the hair follicle shaft and the outer root sheath provides continuation with the epidermis (10). In non-sonicated skin, sucrose can utilise this route to directly diffuse into the dermis. The application of low intensity ultrasound fills the hair follicle shaft with hydrophobic lipids, thus blocking this pathway.

#### Mannitol

Figure 5 presents mannitol permeation curves illustrating the effect of control treatment ( $0 \text{ W cm}^{-2}$ ), low intensity ultrasound ( $0.1 \text{ W cm}^{-2}$ ) and high intensity ultrasound ( $2 \text{ W cm}^{-2}$ ) on drug penetration. Permeation through non-sonicated skin can again be described in terms of three separate phases with short lag-time of less than 0.5 h being followed by a steady-state period of flux  $90.51 \text{ pmol cm}^{-2} \text{ h}^{-1}$  ( $k_p = 5.06 \times 10^{-4} \text{ cm h}^{-1}$  Table 1). From 2.5 h onwards, there is a plateau indicating that drug absorption has ceased; this is due to the evaporation of ethanol and the consequent reduction in the available hydrodynamic force. Interestingly, the mannitol permeability coefficient and the sucrose permeability coefficient are comparable during steady-state, suggesting that the permeation mechanisms

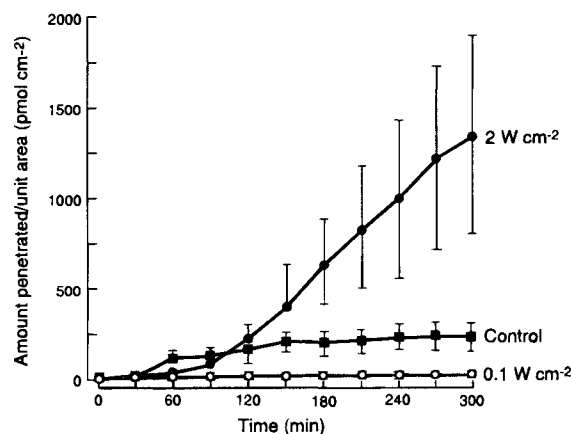


Fig. 5. The effect of presonication on mannitol penetration through rat skin (■, control; ◆,  $0.1 \text{ W cm}^{-2}$ ; ●,  $2 \text{ W cm}^{-2}$ ;  $n = 3$ ).

Table 1. Effect of Low- and High-Intensity Ultrasound (1.1 MHz) on the Penetration of Permeants Through Excised Rat Skin

Permeant	Permeability parameters $\pm$ s. d. ( $J$ , $\text{pmol cm}^{-2} \text{ h}^{-1}$ ; $k_p$ , ( $\times 10^4$ ) $\text{cm h}^{-1}$ ) <sup>a</sup>					
	$0 \text{ W cm}^{-2}$		$0.1 \text{ W cm}^{-2}$		$2 \text{ W cm}^{-2}$	
	$J$	$k_p$	$J$	$k_p$	$J$	$k_p$
Sucrose	$11.49 \pm 3.01$	$6.31 \pm 1.66$	N.D.	N.D.	$51.36 \pm 2.62$	$28.23 \pm 1.44$
Mannitol	$90.51 \pm 19.51$	$5.06 \pm 1.09$	N.D.	N.D.	$375.7 \pm 53.21$	$21.02 \pm 2.98$
Hydrocortisone	$0.105 \pm 0.023$	$1.34 \pm 0.30$	$0.0478 \pm 0.006$	$0.57 \pm 0.077$	$0.81 \pm 0.14$	$10.19 \pm 1.76$
Aminopyrine	$18.03 \pm 1.79$	$7.80 \pm 0.77$	$20.29 \pm 0.80$	$8.77 \pm 0.35$		
5-Fluorouracil	$0.15 \pm 0.03$	$1.13 \pm 0.22$	$0.20 \pm 0.04$	$1.46 \pm 0.29$		

<sup>a</sup> The flux of the drug across the membrane ( $J$ ) is the rate of transport ( $dM/dt$ ) per unit area of membrane and is given by  $J = (dM/dt)/A = D.K.C_d/h$  where  $D$  denotes the diffusion coefficient of the drug in the membrane of thickness  $h$ ,  $K$  is the partition coefficient between donor and membrane and  $C_d$  is the concentration of the drug in the donor solution. The permeability coefficient is  $k_p = D.K/h = J/C_d$ . The lag-time is the time taken for steady-state transport to be reached and depends upon diffusion coefficient and membrane thickness such that  $t_L = h^2/6D$ .

N.D. = value too low for reliable estimation.

may be similar for both agents. However, the mean lag-time for mannitol absorption was shorter than the mean lag time for sucrose absorption possibly because mannitol exhibits a smaller molecular weight than sucrose (182.2 Da versus 342.3 Da).

High intensity ultrasound ( $2 \text{ W cm}^{-2}$ ) degraded the stratum corneum and the flux increased to  $375.67 \text{ pmol cm}^{-2} \text{ h}^{-1}$  ( $k_p = 21.02 \times 10^{-4} \text{ cm h}^{-1}$ ). At this permeation rate, the mannitol in the donor compartment ( $17,874 \text{ pmol}$ ) was progressively depleted and this was manifested in a decreasing penetration rate from 4.5 h onwards. As with sucrose, sonication at a low intensity ( $0.1 \text{ W cm}^{-2}$ ) resulted in the virtual total suppression of mannitol absorption, indicating that this compound primarily penetrates via the hair follicle shafts.

### Hydrocortisone

Figure 6 depicts three absorption profiles, representing control ( $0 \text{ W cm}^{-2}$ ), low intensity ultrasound ( $0.1 \text{ W cm}^{-2}$ ) and high intensity ultrasound ( $2 \text{ W cm}^{-2}$ ). The absorption of hydrocortisone through control skin was essentially biphasic. There was an initial mean lag-time of just under 90 min which was followed by steady-state transport of flux  $0.1049 \text{ pmol cm}^{-2} \text{ h}^{-1}$  ( $k_p = 1.34 \times 10^{-4} \text{ cm h}^{-1}$ ; Table 1). The mechanism of steady-state hydrocortisone absorption is currently uncertain. Traditionally, absorption was thought to be mainly mediated by diffusion through the bulk stratum corneum (11). However, more recent reports have proposed that follicular pathways play a much more important role than previously thought (10,12). The application of high intensity ultrasound ( $2 \text{ W cm}^{-2}$ ) increased hydrocortisone flux to  $0.81 \text{ pmol cm}^{-2} \text{ h}^{-1}$  ( $k_p = 10.19 \times 10^{-4} \text{ cm h}^{-1}$ ) as a consequence of the degradation of the horny layer. A constant penetration rate was sustainable over 5 h since  $78 \text{ pmol}$  of hydrocortisone were initially deposited on the skin surface. However, pre-sonication with this regimen did not produce a shortened mean lag-time. Although the detachment of the stratum corneum increased bulk diffusion, diffusion *via* the shunt pathway was retarded by sebum deposition in the pilosebaceous channels.

Pre-sonication at a low intensity ( $0.1 \text{ W cm}^{-2}$ ) reduced mean hydrocortisone flux to  $0.0478 \text{ pmol cm}^{-2} \text{ h}^{-1}$  ( $k_p = 0.57 \times 10^{-4} \text{ cm h}^{-1}$ ). This is significantly less than the permeability coefficient of control skin ( $P = 0.0208$ , alternate t-test). This

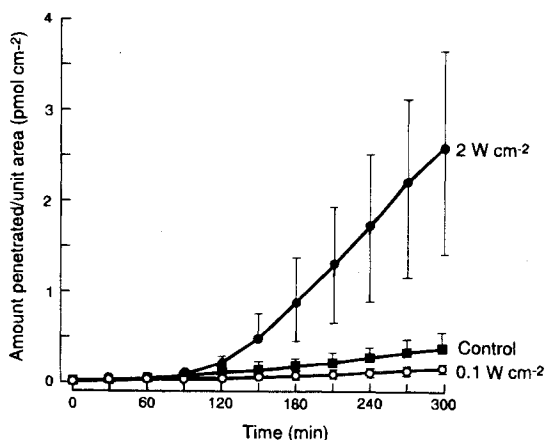


Fig. 6. The effect of pre-sonication on hydrocortisone penetration through rat skin (■, control; ◆,  $0.1 \text{ W cm}^{-2}$ ; ●,  $2 \text{ W cm}^{-2}$ ;  $n = 3$ ).

result suggests that the pilosebaceous route constitutes a major absorptive pathway for hydrocortisone in Wistar rat skin, contributing to about half of total penetration. This estimate compares well with the results derived from published studies involving hairless-rat skin (12). In those experiments, follicle-free skin was grown on the back of the animals and its permeability to hydrocortisone was compared with regular skin. It was determined that the *in vitro* flux through follicle-free skin was approximately 40% of the flux through normal skin. However, for relatively lipophilic compounds such as hydrocortisone, the accumulation of sebum in the hair follicles will merely impede permeation rather than completely suppress it. Therefore, at this stage, the contribution of each pathway in hydrocortisone absorption cannot be precisely ascertained.

### 5-Fluorouracil and Aminopyrine

Pre-sonication at  $0.1 \text{ W cm}^{-2}$  did not significantly affect the penetration profile of either 5-fluorouracil or aminopyrine (Table 1). Since ultrasound exposure blocked the hair follicle shafts with hydrophobic lipids, it may be that no significant penetration of either drug is mediated in rat skin *via* this pathway. It is probable, however, that the extra follicular lipid barrier exerts little influence on more lipophilic entities.

### CONCLUSIONS

The application of high intensity ultrasound ( $1$  to  $2 \text{ W cm}^{-2}$ ) to male Wistar rat skin resulted in the irreversible degradation of the stratum corneum and the dermis. These changes in skin structure were associated with a concomitant reduction in barrier permeability. The damage was intensity-dependent and followed the general patterns observed in the literature reports.

At low intensities ( $0.1$  to  $1 \text{ W cm}^{-2}$ ), sonication resulted in the discharge of sebum from the sebaceous glands into the hair follicle shafts. This is an entirely novel effect. The phenomenon is probably mediated by the mechanical effects of the beam although at higher intensities, ultrasonic heating probably acts as an additional mode of action. The sebum discharge effect has been shown to suppress the transfollicular absorption of some non-lipophilic molecules. Hence, the process is important in phonophoresis where ultrasound is employed to enhance percutaneous drug absorption.

The deposition of sebaceous lipids within the hair follicle shafts means that this absorption pathway is blocked for hydrophilic molecules that penetrate *via* this route. Consequently, this phenomenon has important implications for topical drug delivery in that it can be used as a probe to elucidate the relative follicular contribution to total penetration for these molecules. Presently, there is an urgent need requirement for such a mechanistic tool to aid transdermal delivery research (10). In these *in vitro* rat skin studies, it was found that the highly hydrophilic compounds sucrose ( $\text{Log } P = -2.4$ ) and mannitol ( $\text{Log } P = -2.6$ ) penetrate virtually entirely *via* the pilosebaceous route. The shunt pathway was responsible for approximately half of all hydrocortisone penetration in this model ( $\text{Log } P = 1.55$ ). However, 5-fluorouracil ( $\text{Log } P = -0.95$ ) and aminopyrine ( $\text{Log } P = 0.8$ ) exhibited negligible transfollicular permeation. This set of data indicates that other physico-chemical parameters apart from partition coefficient govern the relative affinity of the permeant for the various pathways of absorption.



Although sebaceous gland histology is similar in most mammals, there are species differences in their gross morphology (13). Furthermore, there are huge site and species differences in the number and surface areas of pilosebaceous units. It has yet to be established whether the sebum discharge effect occurs in regions of human skin that are rich in sebaceous glands. More fundamentally, it is not known whether the process will develop in the *in vivo* situation when other types of ultrasound-tissue interactions such as standing waves, blood cell banding and vasodilation may develop. Consequently, studies to further define this phenomenon are required.

#### ACKNOWLEDGMENTS

We are grateful to Professor R. M. Browne, The School of Dentistry, University of Birmingham for assistance with the staining procedures.

#### REFERENCES

1. V. M. Meidan, A. D. Walmsley, and W. J. Irwin. *Int. J. Pharm.* **118**:130-149 (1995).
2. A. D. Walmsley and C. A. Squier. *J. Dent. Res.* **70**:720 *et seq.* (1991).
3. A. R. Williams. *Ultrasound: Biological Effects and Potential Hazards* (Ed. A. R. Williams) Academic Press, London, 1983.
4. C. P. Robinson. Hydrophones. In: *Output Measurements for Medical Ultrasound* (Ed. R. C. Preston) Springer-Verlag, London, 1991.
5. W. J. Irwin, F. D. Sanderson, and A. Li Wan Po. *Int. J. Pharm.*, **66**:129-140 (1990).
6. T. J. Franz. *J. Invest. Dermatol.* **64**:190-195 (1975).
7. H. S. Gill, S. Freeman, W. J. Irwin, and K. A. Wilson. *Eur. J. Med. Chem.*, **31**:847-859 (1996).
8. O. B. Bayliss. High in: *The Theory and Practice of Histological Techniques 3<sup>rd</sup> Edition* (Eds. J. D. Bancroft and E. Stevens) Churchill-Livingstone, London, 1990.
9. S. Miyazaki, H. Mizuoka, Y. Kohata, and M. Takada. *Chem. Pharm. Bull.* **40**:2826-2830 (1992).
10. A. C. Lauer, L. M. Lieb, C. Ramachandran, G. L. Flynn, and N. D. Weiner. *Pharm. Res.* **12**:179-186 (1995).
11. R. Scheuplein. *J. Invest. Dermatol.* **48**:79-88 (1967).
12. B. Illel, H. Schaefer, J. Wepierre, and O. Doucet. *J. Pharm. Sci.* **80**:424-427 (1991).
13. V. R. Wheatley. *Scand. J. Clin. lab. Invest.* 17 suppl. **85**:11-19 (1965).